Energy 78 (2014) 266–275

Contents lists available at ScienceDirect

Energy

journal homepage: www.elsevier.com/locate/energy

The effects of steam injection on the performance and emission parameters of a Miller cycle diesel engine

Guven Gonca [a, *], Bahri Sahin [a], Adnan Parlak [b], Yasin Ust [a], Vezir Ayhan [c], İdris Cesur [c], Barış Boru [c]

[a] Yildiz Technical University, Naval Arch. and Marine Eng. Department, Besiktas, Istanbul, Turkey
[b] Yildiz Technical University, Marine Eng. Department, Besiktas, Istanbul, Turkey
[c] Sakarya University, Technical Education Faculty, Sakarya, Turkey

ARTICLE INFO

Article history:
Received 20 June 2014
Received in revised form
25 September 2014
Accepted 3 October 2014
Available online 13 November 2014

Keywords:
Diesel engine
Steam injection method
Miller cycle
Engine performance
NOx emissions
Two-zone combustion model

ABSTRACT

The application of the Miller cycle into the internal combustion engines is proposed to decrease NOx emissions, in the recent years. Another NOx control technique is the steam injection method (SIM). In this study, the application of these methods together into a single cylinder, direct injection diesel engine is experimentally and theoretically performed. Two different Miller cycles, which provide 5 and 10 crank angle (CA) retarding compared to standard condition, are applied with two different camshafts. SIM is applied at three different injection rates which are 10%, 20% and 30% of the fuel mass. The results obtained are compared with standard conditions in terms of the performance and emissions. The simulation results are verified with experimental data with non-notable errors. In the experimental results, NO and CO_2 emissions decreased up to 48% and 2.2%; HC and CO emissions increased by 46% and 34% with the penalty by 6.4% and 9.2% for the effective power and efficiency. The optimum condition has been defined as 10 CA retarding and 30% steam injection rate (C62-S30) in terms of the maximum NO reduction. The results demonstrate that the combination can be applied into the diesel engines to minimize NO and CO_2 emissions.

1. Introduction

In the recent years, the application of the Miller cycle into the internal combustion engines has been become widespread in the engine researchers. This method provides a high decrease rate in the formation of NOx emissions [1–9]. Another technique is the SIM (steam injection method) which has been recently developed to decrease NOx emissions released from internal combustion engines [19–22]. In order to obtain maximum NOx reduction rate, the combination of these two methods may be used in the diesel engines.

Wang et al. [1] experimentally reduced NOx emissions by applying the Miller cycle into a diesel engine. Wang et al. [2,3] carried out an experimental [2] and an analytical [3] study on the Miller Cycle Otto Engine with late intake valve closing version in order to decrease NOx emissions from a petrol engine. Miller cycle decreased the compression pressure and temperature in the cylinder at the end of compression stroke. Thus, lower exhaust temperature and less NOx formation were seen compared to those of standard Otto cycle.

Mikalsen et al. [4] investigated the feasibility and potential advantages of the application of the Miller cycle into a small scale Otto cycle natural gas engine by using multidimensional simulation for a combined heat and power system. As a result, the SFC (specific fuel consumption) of the engine was reduced with the cost of a decreased power to weight ratio. Gonca et al. [5–8] computationally demonstrated that the application of Miller cycle into a diesel engine could abate the NO emissions and increase the effective efficiency. Sarkhi et al. [9–11] investigated the effects of the variable specific heats of the working fluid on the performance for an air standard reversible Miller cycle [9] and irreversible Miller cycle [10]. In another study, Sarkhi et al. [11] analyzed the cycle performance by using the maximum power density criteria. Zhao and Chen [12] conducted a performance analysis for an-air standard irreversible Miller cycle with respect to the change of the pressure ratios. Ebrahimi [13] analyzed an air standard reversible Miller cycle with respect to variation of engine speed and variable specific heat ratio of working fluid and Ebrahimi [14] analyzed an air

* Corresponding author. Tel.: +90 212 383 2950; fax: +90 212 383 2941.
E-mail address: ggonca@yildiz.edu.tr (G. Gonca).

http://dx.doi.org/10.1016/j.energy.2014.10.002
0360-5442/

Nomenclature

A	heat transfer area (cm^2)
C_v	constant volume specific heat (kJ/kg K)
C_p	constant pressure specific heat (kJ/kg K)
C	blow by coefficient
B	bore (cm)
F	fuel–air ratio
h	specific enthalpy (kJ/kg)
h_{tr}	heat transfer coefficient (W/m^2K) of burnt and unburnt zones
H	enthalpy (kJ/kg)
H_u	low heat value of the fuel (kJ/kg)
m	mass (g)
$\dot{m}$	time-dependent mass rate (g/s)
M	molecular weight (g)
n	injection constant
P	pressure (bar)
Q	loss heat passed through the cylinder wall (J)
$\dot{Q}$	rate of heat transfer (J/s)
RGF	residual gas fraction
s	specific entropy (kJ/kg K)
S	stroke (cm)
T	temperature (K)
u	specific internal energy (kJ/kg)
v	specific volume (cm^3/g)
V	volume (cm^3)
W	work output (J)
x	burn fraction
$\dot{x}_i$	fraction rate of the total injected fuel mass

Greek letters

ε	ratio of half stroke to rod length
ϕ	equivalence ratio
$\Gamma(n)$	gamma function
θ	crank angle (degree)
τ	time (ms)
ω	angular velocity (rad/s)

Subscripts

a	air
b	burned zone
cyl	cylinder
di	injection duration parameter
dif	diffusive combustion phase
f	fuel
fi	injected fuel
id	ignition delay(ms)
l	leak, loss
pre	premixed combustion phase
r	reference
si	start of fuel injection (degree)
st	stoichiometric
u	unburned zone
w	cylinder walls

standard irreversible Miller cycle with respect to the variation of relative air–fuel ratio and stroke length based on finite-time thermodynamics. The power output and thermal efficiency were obtained by introducing the compression ratio, air–fuel ratio and stroke length. It was illustrated that the power output and thermal efficiency of the cycle reach to maximum point with certain values of the compression ratio. Rinaldini et al. [15] carried out an experimental and numerical study by using KIVA which is a CFD based code. They assessed the potential and the limits of the Miller cycle application into a High Speed Direct Injection (HSDI) Diesel engine in terms of abating NOx and soot. It was shown in the results that when the Miller cycle is applied to a diesel engine, NOx and soot emissions could be reduced up to 25% and 60%, respectively. Li et al. [16] experimentally examined the effects of the Miller cycle with early and late intake valve closing (EIVC and LIVC) versions on the brake specific fuel consumption (BSFC) of a boosted direct injection (DI) gasoline engine. At the high load conditions, the fuel economy is improved up to 4.7% with LIVC; however, a considerable change was not seen in SFC with EIVC version. At the low load conditions, SFC is improved up to 6.8% and 7.4% with LIVC and EIVC versions, respectively. Wu et al. [17] studied on the analysis of a supercharged Miller cycle Otto engine with EIVC version. Ge et al. [18] examined the influences of heat transfer and friction losses on the performance of an air standard Miller cycle based on finite-time thermodynamics.

The steam injected method firstly was proposed by Parlak et al. [19]. This method yielded lower NOx emissions by 33% compared to standard condition for a single cylinder, naturally aspirated diesel engine. Also, the engine performance increased up to 3%. Kokkulunk et al. [20,33] investigated the effects of steam injection and EGR applications on the engine performance and NO emission of a direct injection diesel engine. Gonca et al. [5,6] conducted a theoretical study to compare the steam injected diesel engine and the Miller cycle diesel engine using two-zone combustion model. It was observed from the results that the Miller cycle and steam injection decrease the NO emissions at high rates. Cesur et al. [21] and Kokkulunk et al. [22] applied steam injection method into gasoline and diesel engines; they observed a reduction in NOx emissions and a increment in engine performance. Gonca et al. [23] studied on determination of the optimum steam temperatures and optimum steam mass ratios for turbocharged internal combustion engines.

Gonca [24] applied the SIM into a diesel engine fueled with the diesel–ethanol blend. The results showed that the method could improve the engine performance and decrease NO emissions. Parlak et al. [25] investigated the influences of the steam injection on a diesel engine fueled with tobacco seed oil methyl ester.

In this study, the influences of the application of the Miller cycle and steam injection on the performance and emission outputs for a naturally aspirated direct injection single cylinder diesel engine have been examined experimentally and theoretically. Engine torque, effective power, effective efficiency, SFC and the NO, CO, CO_2 and HC emissions have been experimentally obtained. The experimental results have been compared with the results of two-zone combustion model and a good approximation has been obtained with non-prominent errors. There is no study like this including the application of the Miller cycle and steam injection together, in the literature. Apart from former studies in the literature, this study also includes a comprehensive comparison of theoretical and experimental results for a steam injected and Miller cycle diesel engine.

2. Materials and method

2.1. Experimental set-up

The experiments were performed with a single cylinder, four-stroke and direct injection (DI) diesel engine. Table 1 demonstrates the engine properties. The Miller cycles are provided by retarding the closing of intake valve as 5 and 10 CA (crank angle). The original

Table 1
Engine properties [34].

Engine type	Antor
Bore [mm]	85
Stroke [mm]	90
Cylinder number	1
Stroke volume [dm^3]	0.51
Power, 2700 rpm [kW]	9
Injection pressure [bar]	175
Injecting timing [crank angle]	28
Compression ratio	17.5
Maximum speed [rpm]	3000
Cooling	Air
Injection	Direct injection

camshaft is camshaft 52 (STD) which means the intake valve is closed 52 CA after the bottom dead center (BDC). 5, and 10 CA retarding are conducted with camshaft 57 (C57) and camshaft 62 (C62). In order to apply the Miller cycle into the diesel engine, two different cam shafts were manufactured and mounted into the engine one by one. The picture of the cam shafts and technical drawing are given in Fig. 1.

In order to apply steam injection into the diesel engine, electronically controlled steam injection system developed by Parlak et al. [19] was used. In the previous studies [19–22,25,33], the researchers used the waste exhaust heat from waste heat boiler to produce steam. However, this method takes long time and it was proven that the exhaust enthalpy is enough to obtain sufficient

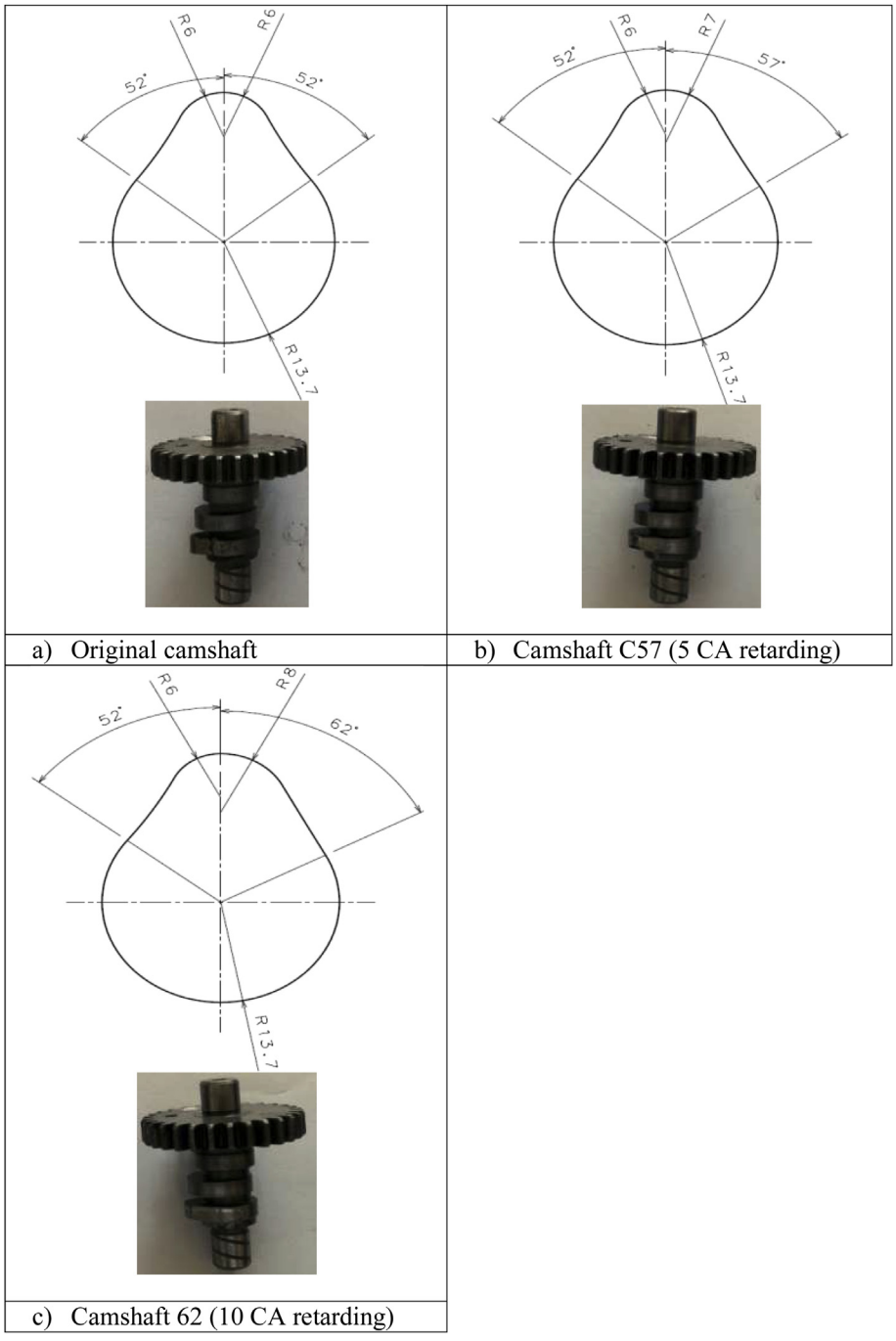

Fig. 1. The picture and technical drawings of the original and modified camshafts in accordance with the Miller cycle.

steam mass. Therefore, a boiler with electric resistance is used to acquire steam at steady condition in the shortest time. The boiler is demonstrated in Fig. 2. The steam in the boiler, which is kept in the form of saturated water with conditions of 3 bar and 133.5 °C, is injected with an injector which is positioned at the back of intake valve in the manifold. The saturated water is transformed the superheated vapor due to lower in-cylinder pressure after injection. 10%, 20% and 30% steam ratios of fuel mass were injected into the cylinder. The steam injection system and experimental set-up are shown in Fig. 3.

In order to measure brake torque, the engine is coupled with an electric dynamometer of 20 kW absorbing capacity using an "S" type load cell with the precision of 0.01 kg. In order to measure species of the exhaust emissions, MRU Spectra 1600 L type gas analyzer has been used. CO, CO_2, NO, and HC emissions have been obtained as unit of (%) and ppm.

In this study, in-cylinder pressure has been measured by Kistler brand 6061B model, piezo-electric sensor and Kistler 5018 type charge amplifier. The data transfer has been carried out by SMETEC brand data card which has 1 Mbyte data signaling rate from single channel "Combi Combustion Indication System". The angular position of the piston with respect to crank angle has been acquired using Koyo TRD J1000-RZ type encoder which has 1000 pulse/revolution.

The experiments were performed at variable engine speeds 1500, 1800, 2100, 2400, 2700 and 3000 rpm and full load condition.

Fig. 2. The steam boiler.

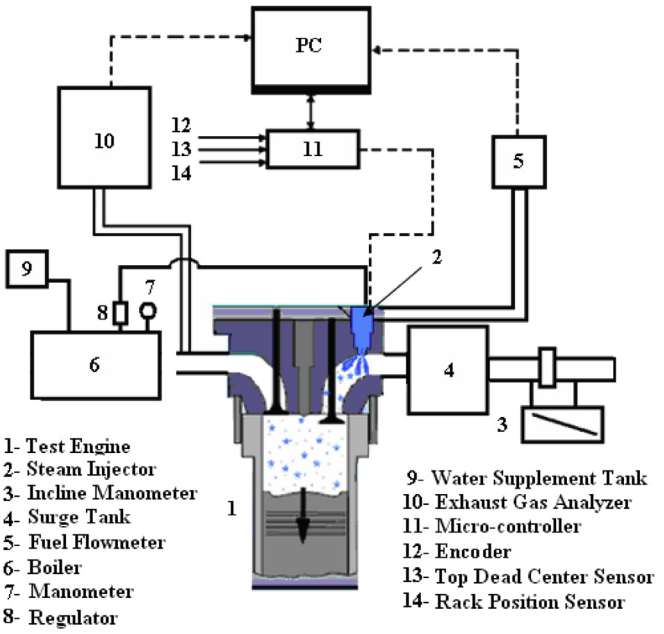

Fig. 3. Experimental set-up [26].

In order to compare, standard camshaft was used for the naturally aspirated conditions at initial and then the other camshafts which provide the Miller cycle were mounted into the engine at the different steam injection conditions (10%, 20% and 30% steam ratios of fuel mass). The experiments were repeated three times for each camshaft and steam injection ratio and then performance and emission data were compared with those of standard camshaft and without steam injection condition. Total uncertainties of the measured parameters are substantial to verify the accuracy of the test results, so they are given in Table 2.

2.2. Theoretical model

Combustion simulation of diesel engine is conducted by using two-zone combustion model to calculate NO emission, torque, effective power, effective efficiency and specific fuel consumption. In this two-zone combustion model [5,6,24,33,34], the gas region are divided in two zone as burned and unburned gas regions.

The injected fuel reacts with the air in the unburned region and becomes a part of the burnt gas region by combustion. In the cylinder, the equation of the energy conservation in differential form may be given as:

Table 2
The errors in parameters and total uncertainties [34].

Parameters	Systematic errors ±
Load [N]	0.1
Speed [rpm]	1.0
Time [s]	0.1
Temperature [°C]	1.0
Fuel consumption [g]	0.01
NO [ppm]	5% of measured value
HC [ppm]	5% of measured value
CO [%]	5% of measured value
CO_2 [%]	5% of measured value
SFC [g/kWh]	1.5
Torque [Nm]	1.1

$$m\frac{du}{d\theta}+u\frac{dm}{d\theta}=-\frac{dQ_b}{d\theta}-\frac{dQ_u}{d\theta}-P\frac{dV}{d\theta}+\frac{dm_{fi}}{d\theta}h_{fi}-\frac{dm_l}{d\theta}h_l \tag{1}$$

where m_l is leak mass and m_{fi} is mass of injected fuel; h_{fi} and h_l are enthalpies of fuel injected and leak mass respectively. The first term of the left side of the equation is the internal energy rate and the second term is the mass rate depending on crank angle. The heat transfers from burned and unburned zone are expressed, respectively as:

$$\dot{Q}_b=h_{tr}A_bT_{bw} \tag{2}$$

$$\dot{Q}_u=h_{tr}A_uT_{uw} \tag{3}$$

where $T_{uw}=T_u-T_w$ and $T_{bw}=T_b-T_w$, h_{tr} is heat transfer coefficient of burned and unburned gas zones, A_b and A_u are the areas of burned and unburned gas inside the cylinder which are in contact with the cylinder walls and T_b, T_u and T_w are the temperatures of the burned gas zone, unburned gas zone and cylinder walls. The change of stroke volume depending on crank angle is:

$$\frac{dV}{d\theta}=\frac{\pi}{8}B^2S\,\mathrm{Sin}\,\theta\left[1+\varepsilon\frac{\cos\theta}{(1-\varepsilon^2\sin^2\theta)^{\frac{1}{2}}}\right] \tag{4}$$

In order to solve the differential equations, the following expressions are used in the model.

Internal energy:

$$\frac{du}{d\theta}=C_p-\frac{Pv}{T}\left(\frac{\partial\ln v}{\partial\ln T}\right)_P\frac{dT}{d\theta}-v\left[\frac{\partial\ln v}{\partial\ln T}+\frac{\partial\ln v}{\partial\ln P}\right]_T\frac{dP}{d\theta}+\frac{\partial u}{\partial\phi}\frac{d\phi}{d\theta} \tag{5}$$

The burned gas leaking through the rings:

$$\frac{dm_l}{d\theta}=\frac{Cm}{\omega} \tag{6}$$

where C and ω are blow by coefficient and angular velocity, respectively. The mass balance inside the cylinder can be expressed as:

$$m=m_a+m_{fi} \tag{7}$$

where m_a and m_{fi} are the masses of the air and injected fuel respectively. If Eq. (7) is written in differential form, it becomes:

$$\frac{dm}{d\theta}=\frac{dm_a}{d\theta}+\frac{dm_{fi}}{d\theta} \tag{8}$$

The air and injected fuel rates changing with crank angle within the cylinder are expressed respectively as:

$$\frac{dm_a}{d\theta}=\frac{-\dot{m}_l/\omega}{1+\phi F_{st}}=\frac{-Cm_a}{\omega} \tag{9}$$

$$\frac{dm_{fi}}{d\theta}=\frac{1}{\omega}\left(\dot{m}_{fi}-\frac{\dot{m}_l\phi F_{st}}{1+\phi F_{st}}\right)=\frac{\dot{m}_{fi}-Cm_{fi}}{\omega} \tag{10}$$

where $\dot{m}_l$, ϕ and F_s are the time-dependent gas leak rate, the equivalence ratio and the stoichiometric fuel–air ratio by mass, respectively. $\dot{m}_{fi}$ is the time-dependent fuel injected rate and can be expressed as:

$$\dot{m}_{fi}=\dot{x}_im_{fi} \tag{11}$$

where m_{fi} and $\dot{x}_i$ are the total mass of the fuel to be injected and fraction rate of the total injected fuel mass respectively, which can be given as:

$$m_{fi}=\phi F_{st}\left(1-\mathrm{RGF}\right)m_a \tag{12}$$

$$\dot{x}_i=\frac{\omega}{\theta_{di}\Gamma(n)}\left(\frac{\theta-\theta_{si}}{\theta_{di}}\right)^{n-1}\exp\left[\frac{-(\theta-\theta_{si})}{\theta_{di}}\right] \tag{13}$$

where $\Gamma(n)$ is the gamma function [27], θ_{di} is a parameter of injection duration and θ_{si} is the start of fuel injection. The gamma function is derived as:

$$\ln\Gamma(n)=\left(n-\frac{1}{2}\right)\ln(n)-n+\frac{1}{2}\ln(2\pi)+\frac{1}{12n}-\frac{1}{360n^3}+\frac{1}{1260n^5}-\frac{1}{1680n^7} \tag{14}$$

The values of n could be taken for the diesel engine with open chamber as $1\le n\le 2$ and for close chamber as $3\le n\le 5$ but exact value is dependent on fuel used and engine design [27]. Differential equation systems used in the calculation of the processes that consist during the period from the beginning of the compression to the end of the expansion process are given in Eqs. (15)–(20) [5,6,24,33,34].

The time (crank angle)-dependent expressions of pressure, burned and unburned gas temperatures, work, heat leak and heat loss are given respectively as:

$$\frac{dP}{d\theta}=\frac{\begin{array}{l}\frac{C}{\omega}\left(\frac{V}{m}+\frac{\vartheta_1}{C_{p,b}T_b}\left(\left(x^2-x\right)(h_b-h_u)\right)\right)+\frac{h_{tr}}{\omega m}A_{cyl}\left(\sqrt{x}\,\frac{\vartheta_1}{C_{p,b}T_b}T_{bw}+(1-\sqrt{x})T_{uw}\frac{\vartheta_2}{C_{p,u}T_u}\right)\\ +\left(\frac{\vartheta_1}{C_{p,b}T_b}(h_b-h_u)-(v_b-v_u)\right)\frac{dx}{d\theta}+\frac{1}{m}\frac{dV}{d\theta}+\left(\frac{\vartheta_1}{mC_{p,b}T_b}(xh_b-(1-x)h_u)-H_u-\frac{V}{m^2}\right)\frac{dm_{fi}}{d\theta}\\ +(1-x)\left(\frac{\vartheta_1}{C_{p,b}T_b}\left(-T_u\frac{ds_u}{d\theta}+P\frac{dv_u}{d\theta}+\frac{du_u}{d\theta}\right)-\frac{dv_u}{d\theta}+\frac{\vartheta_2}{C_{p,u}}\frac{ds_u}{d\theta}\right)\frac{d\phi}{d\theta}+x\left(\frac{\vartheta_1}{C_{p,b}T_b}\left(P\frac{dv_b}{d\theta}+\frac{du_b}{d\theta}\right)-\frac{dv_b}{d\theta}\right)\frac{d\phi}{d\theta}\end{array}}{x\left(\frac{\vartheta_1}{C_{p,b}T_b}+\frac{\vartheta_3}{P}\right)+(1-x)\left(\frac{\vartheta_2^2}{C_{p,u}T_u}+\frac{\vartheta_4}{P}\right)} \tag{15}$$

where x, H_u, A_{cyl} are the burning fraction, lower heating value of fuel and heat transfer area of the cylinder. $C_{p,b}, C_{p,u}; v_b, v_u; s_b, s_u; h_b, h_u$ are specific heat at constant pressure,

specific volume, specific entropy and specific enthalpy for the burned and unburned zones respectively.

$$\vartheta_1 = \frac{\partial In\, v_b}{\partial In\, T_b} v_b, \quad \vartheta_2 = \frac{\partial In\, v_u}{\partial In\, T_u} v_u$$

$$\vartheta_3 = \frac{\partial In\, v_b}{\partial In\, P} v_b, \quad \vartheta_4 = \frac{\partial In\, v_u}{\partial In\, P} v_u$$

$$\frac{dT_b}{d\theta} = \frac{1}{C_{p,b}}\left(-\frac{h_{tr}}{\omega m} A_{cyl} \frac{1}{\sqrt{x}} T_{bw} + \vartheta_1 \frac{dP}{d\theta}\right) \tag{16}$$

$$\frac{dT_u}{d\theta} = -\frac{h_{tr}}{\omega m C_{pu}} A_{cyl} \frac{T_{uw}}{1+\sqrt{x}} + \frac{\vartheta_2}{C_{pu}} \frac{dP}{d\theta} - \frac{\partial s_b}{\partial \phi} \frac{d\phi}{d\theta} \frac{1}{C_{pb}} \tag{17}$$

$$\frac{dW}{d\theta} = -P\frac{dV}{d\theta} \tag{18}$$

$$\frac{dH_l}{d\theta} = \frac{Cm}{\omega}\left[\left(1-x^2\right)h_u + x^2 h_b\right] \tag{19}$$

$$\frac{dQ_l}{d\theta} = \frac{h_{tr}}{\omega} A_{cyl}\left[\sqrt{x}T_{bw} + (1-\sqrt{x})T_{uw}\right] \tag{20}$$

Hohenberg [28] gives the coefficient of the heat transfer (h_{tr}) as below:

$$h_{tr} = C_1 V^{-0.06} P^{0.8} (xT_b + (1-x)T_u)^{-0.4}\left(\bar{S}_p + C_2\right)^{0.8} \tag{21}$$

where $\bar{S}_p$ is mean piston velocity in meters per second, $C_1 = 130$ and $C_2 = 1.4$ respectively. Sitkei [29] correlation is used to calculate ignition delay and it is written as following:

$$\tau_{id} = 0.5 + 0.1332P^{-0.7} e^{\frac{3.92782}{T}} + 4.637P^{-1.8} e^{\frac{3.92782}{T}} \tag{22}$$

where P and T are average temperature and pressure of during the ignition delay. Dual Wiebe function states the burn fraction and x versus crank angle is used to express the heat release from combustion and determined as following [30]:

$$x = a_v\left[Q_{pre}\left(1 - e^{-a_v\left(\frac{\theta}{\theta_{pre}}\right)^{(m_{pre}+1)}}\right) + Q_{dif}\left(1 - e^{-a_v\left(\frac{\theta}{\theta_{dif}}\right)^{(m_{dif}+1)}}\right)\right] \tag{23}$$

where Q_{pre} and Q_{dif} are heat release rate of premixed and diffusive combustion. x is 0 at the beginning of the combustion and x becomes 1 at the end of the combustion. It can be rewritten by differentiating with respect to crank angle:

$$\frac{dx}{d\theta} = a_v\left[\frac{Q_{pre}}{\theta_{pre}}(m_{pre}+1)\left(\frac{\theta}{\theta_{pre}}\right)^{m_{pre}} e^{-a_v\left(\frac{\theta}{\theta_{pre}}\right)^{(m_{pre}+1)}} + \frac{Q_{dif}}{\theta_{dif}}\left(m_{dif}+1\right)\left(\frac{\theta}{\theta_{dif}}\right)^{m_{dif}} e^{-a_v\left(\frac{\theta}{\theta_{dif}}\right)^{(m_{dif}+1)}}\right] \tag{24}$$

$$\theta = \theta_r - \theta_b \tag{25}$$

where θ_r and θ_b are reference crank angle and start angle of combustion respectively, a_v, m_{pre}, θ_{pre}, m_{dif}, θ_{dif} are Wiebe constants in the premixed and diffusive combustion conditions.

NO emissions are calculated by using extended Zeldovich mechanism taking into account 10 combustion products including (CO_2, H_2O, N_2, O_2, CO, H_2, H,O, OH,NO). In this study the ECP code which is developed by Olikara and Borman [32] is modified by adding steam injection into the reactants [6,20–24,33]. The combustion reaction used in the modified code is expressed as below:

$$\varepsilon\phi(C_\alpha H_\beta O_\gamma N_\delta) + (0.21O_2 + 0.79N_2) + xH_2O \rightarrow \nu_1 CO_2 + \nu_2 H_2O + \nu_3 N_2 + \nu_4 O_2 + \nu_5 CO + \nu_6 H_2 + \nu_7 H + \nu_8 O + \nu_9 OH + \nu_{10} NO \tag{26}$$

3. Results and discussion

Fig. 4 shows the engine torque and effective power with respect to change of engine speed for different camshafts and steam injection ratios. It is clear from the figures that the engine torque reduces and effective power increases with increasing engine speed, the effective power increases until 2700 rpm and then starts to reduce. The application of the steam injection and the Miller cycle into the diesel engine decreases the torque and effective power. The maximum decrease rate in the engine torque is obtained with C63-S30, as 6.4% at 3000 rpm, the minimum reduction rate in effective power is seen with C57-S10, as 0.2% at 1500 rpm. The minimum torque and minimum effective power are 25.1 Nm and 5.34 kW with C62-S30 at 3000 rpm and 1500 rpm, respectively.

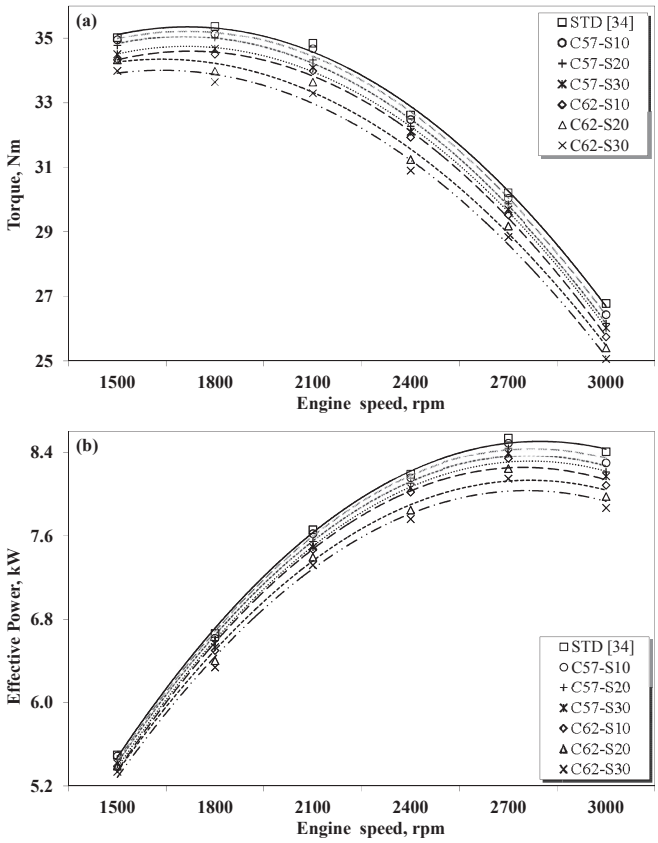

Fig. 4. a) Torque and b) effective efficiency with respect to engine speed for different camshaft and turbo charging modes.

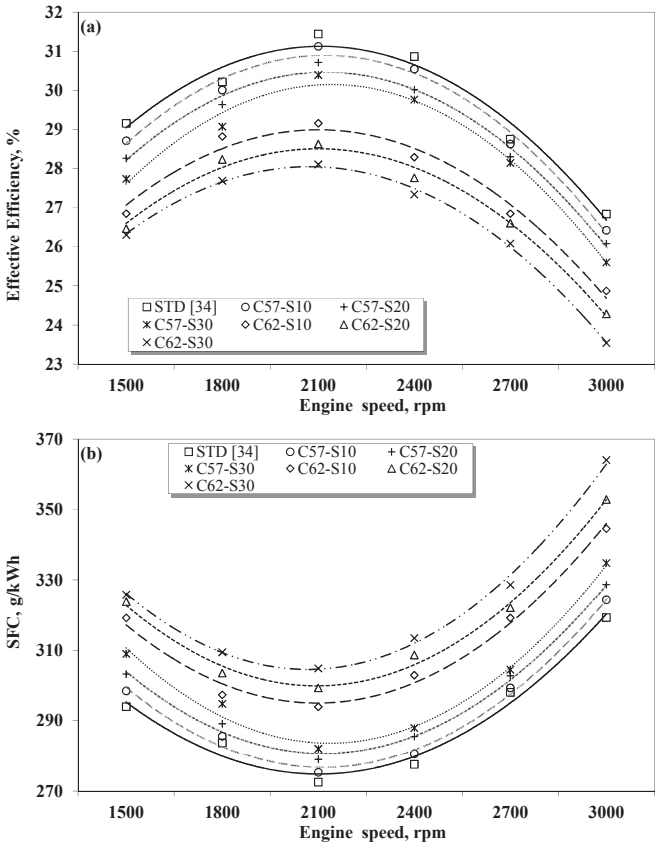

Fig. 5. a) Effective efficiency and b) SFC with respect to engine speed for different camshaft and turbo charging modes.

The change of the effective efficiency and specific fuel consumption (SFC) with respect to engine speed for different camshafts and steam injection ratios are illustrated in Fig. 5. It is obviously seen from the figures that the middle range of the engine speeds gives the maximum effective efficiency and the minimum SFC. At the lower and higher engine speeds, the effective efficiency and SFC are worsened. The application of the Miller cycle and steam injection decreases the effective efficiency and SFC. The maximum reduction rate is obtained with C62-S30, as 12.3% at 3000 rpm, the minimum reduction rate is seen with C57-S10, as 0.5% at 2700 rpm for the effective efficiency. The minimum effective efficiency and maximum SFC are obtained with C62-S30, as 23.5% and 364 g/kWh at 3000 rpm for the steam injected and Miller cycle conditions.

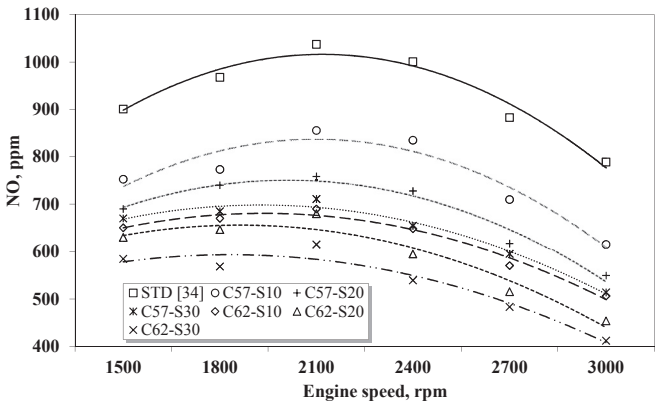

Fig. 6. NO emissions with respect to engine speed for different camshaft and turbo charging modes.

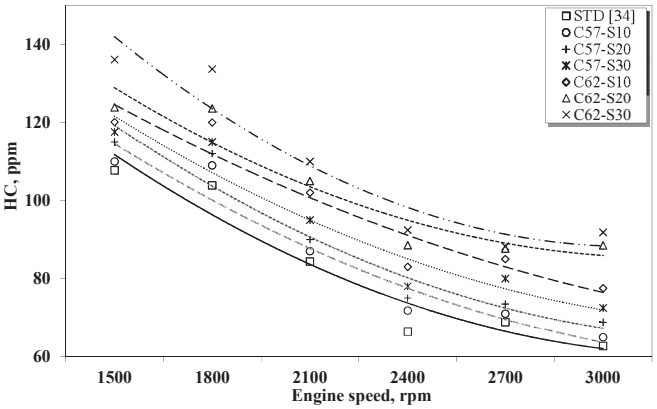

Fig. 7. HC emissions with respect to engine speed for different camshaft and turbo charging modes.

Fig. 6 illustrates the variation of NO formation with respect to engine speed for different camshafts and steam injection modes. The formation of NO emission is very sensitive to combustion temperature and duration [21,22]. The maximum NO formation is seen at stochiometric combustion conditions in which equivalence ratio is 1. At the lower and higher equivalence ratios, the formation of NO slows down. Also, the equivalence ratio affects the combustion temperature, the maximum combustion temperatures are seen about stochiometric combustion conditions [31]. It can be observed from Fig. 6 that the maximum NO formation is seen in the medium engine speeds owing to the combination of these effects at all conditions.

The application of the Miller cycle and steam injection method leads to reduction in the NO formation at the all engine speeds. The maximum and minimum NO reduction rates are seen as 48% with C62-S30 at 3000 rpm and as %16 with C57-S10 at 1500 rpm. The minimum and maximum NO quantities are found as 412 ppm with C62-S30 at 3000 rpm and 856 ppm with C57-S10 at 2100 rpm, respectively.

Fig. 7 demonstrates the variation of HC with respect to engine speed. HC formation rate decreases with increasing engine speeds due to leaner combustion conditions for all engine modes. HC emission raises considerably with the increasing steam injection

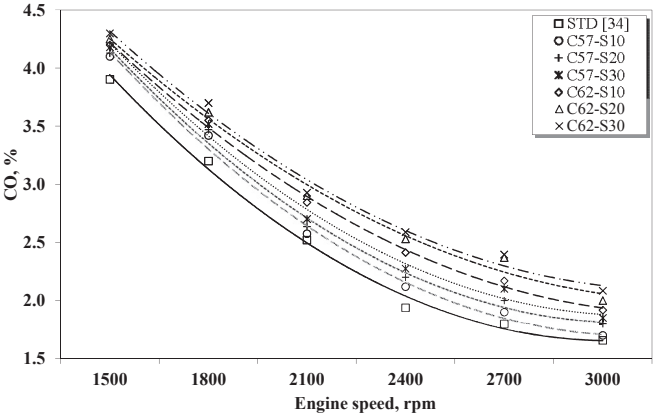

Fig. 8. CO emissions with respect to engine speed for different camshaft and turbo charging modes.

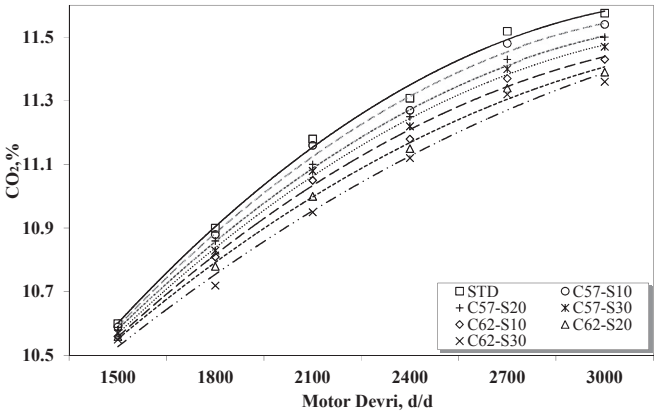

Fig. 9. CO_2 emissions with respect to engine speed for different camshaft and turbo charging modes.

ratio and Miller cycle angle (retarding angle), because they lead to lower oxygen concentration, lower volumetric efficiency and higher equivalence ratio. As expected, the highest HC levels are observed with the C62-S30. The maximum and minimum increment rates are 46% with C62-S30 at 3000 rpm and 2% with C57-S10 at 1500 rpm, respectively. The maximum HC is 136 ppm with C62-S30 at 1500 rpm and the minimum HC is 65 ppm with C57-S10 at 3000 rpm for the Miller cycle and steam injected conditions.

Fig. 8 shows the variation of CO with respect to engine speed. The formation characteristics of CO are similar to those of HC emissions, the formation of CO and HC emissions strongly depends on oxygen concentration (equivalence ratio) of the cylinder charge, hence CO formation rate decreases with increasing engine speeds. However, it increases with the application of the Miller cycle and steam injection method. The highest CO levels are seen with the C62-S30. The maximum CO is 4.18% with C62-S30 at 1500 rpm and the minimum CO is 1.7% with C57-S10 at 3000 rpm for the Miller cycle and steam injection conditions. The maximum and minimum increment rates are 34% with C62-S30 at 2400 rpm and 2% with C57-S10 at 2100 rpm, respectively.

The variation of CO_2 with respect to engine speed is shown in Fig. 9. CO_2 emissions are complete combustion products so it increases with the increment of oxygen concentration and

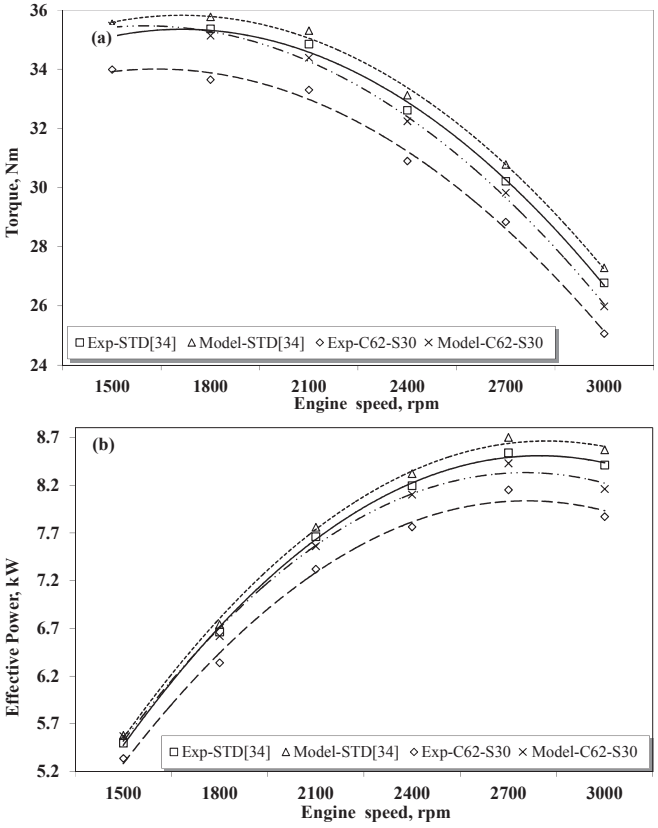

Fig. 10. Comparison of theoretical and experimental data of a) torque and b) effective power.

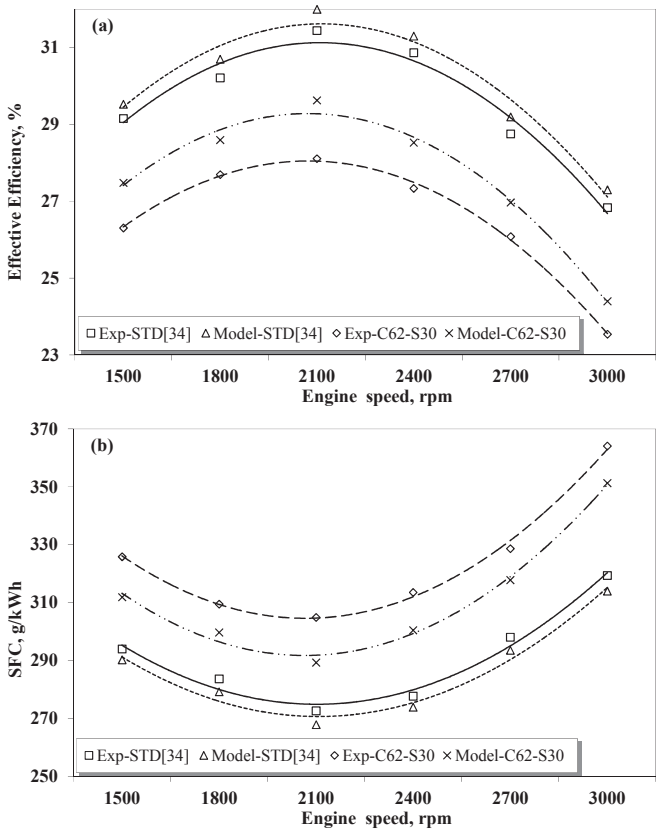

Fig. 11. Comparison of theoretical and experimental data of a) effective efficiency and b) SFC.

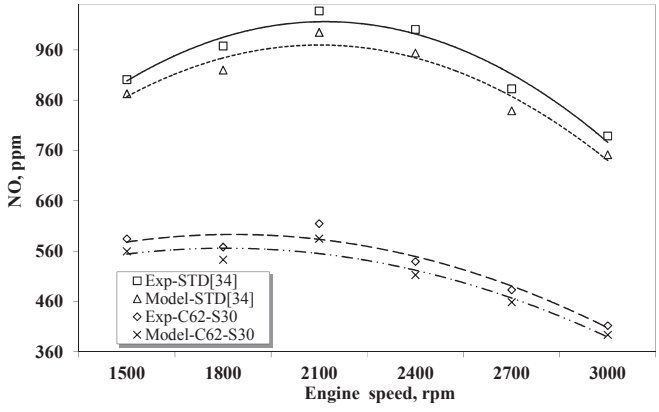

Fig. 12. Comparison of theoretical and experimental data of NO formation.

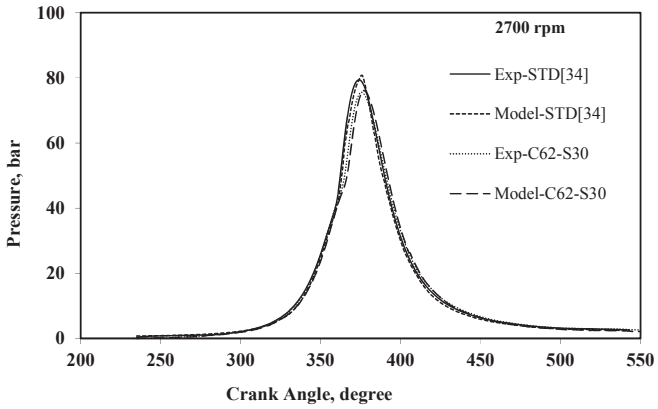

Fig. 13. Comparison of theoretical and experimental data for cylinder pressure.

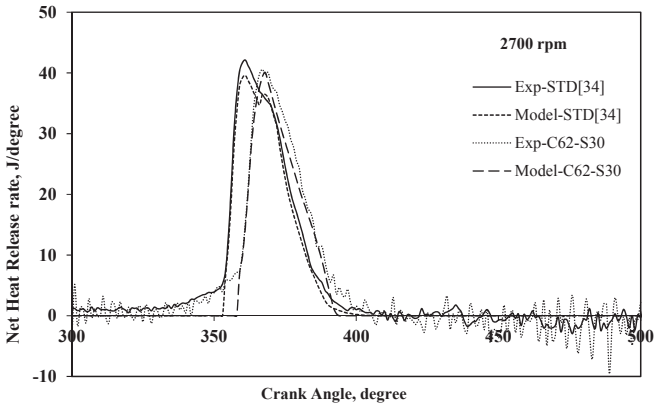

Fig. 15. Comparison of theoretical and experimental data for net heat release rate.

combustion temperatures. It increases with increasing engine speed as oxygen concentration and combustion temperatures rise up. On the other hand, CO_2 decreases with increasing steam ratios and retarding angles since oxygen concentration and combustion temperatures reduce depending on volumetric efficiency. The maximum and minimum CO_2 reduction rates are seen as 2.1% with C62-S30 at 2100 rpm and as %0.2 with C57-S10 at 1500 rpm. The maximum and minimum CO_2 are found as 11.36% with C62-S30 at 3000 rpm and 10.59% with C57-S10 at 1500 rpm, respectively.

The main purpose of this study is to decrease NO emission. C62-S30 condition gives the maximum NO reduction rates compared to other engine modes. Therefore, C62-S30 condition has been selected for the comparison of the experimental and theoretical results in the following figures. When we investigate Figs. 10–12, we see that theoretical results agree with experimental data pretty well and there is no notable error. It is clear that torque, effective power, effective efficiency and NO decrease and SFC increases by the application of the Miller cycle and SIM together.

Figs. 13–15 demonstrate the comparison of theoretical and experimental data for cylinder pressure, temperature and net heat release rate. It is obvious that the maximum cylinder pressure and net heat release rate remarkably decrease, ignition delay slightly increases however, in-cylinder temperatures minimize with the application of the Miller cycle and steam injection method. If we compare Figs. 12 and 14, we see that NO emissions decrease with reducing peak combustion temperatures as expected.

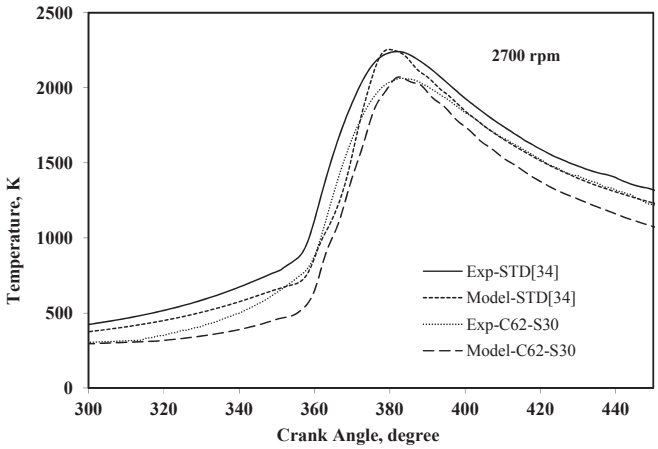

Fig. 14. Comparison of theoretical and experimental data for cylinder temperature.

4. Conclusion

In this study, the application of the Miller cycle and SIM into a diesel engine has been performed and the effects of this application on the engine performance and emissions have been theoretically and experimentally examined. The torque, effective power and effective efficiency are considerably reduced by applying the combination of the Miller cycle and SIM together. NO and CO_2 emissions decrease, CO and HC emissions increased at all engine speeds compared to the standard conditions. Theoretical study has been conducted by using two-zone combustion model. Theoretical model results have been verified with non-remarkable errors in terms of torque, effective power and efficiency, SFC and NO emissions. Even though the maximum performance decreases, C62-S30 gives the lowest NO emissions, therefore theoretical and experimental data comparisons are conducted at C62-S30 conditions, as this study primarily aims to decrease NO emissions. It is known that although the application of the Miller cycle into an internal combustion engine decrease NO emission, a reduction is seen in the torque [1–9]. The application of the SIM and the Miller cycle together decreases the torque and NO emissions compared to standard conditions. The maximum reduction rates in NO are obtained with C62-S30 conditions. NO emissions decrease by 48%; the torque and the effective efficiency decreases up to 6.4% and 9.2%; HC and CO increased up to 46% and 34%, however a reduction is seen in the CO_2 emissions by 2.2%. It is clear in the results that the application of the Miller cycle and SIM together decreases NO emissions in high rates, thus, this combination may be used in the diesel engines so as to lower the formation of NO emissions.

Acknowledgment

This study is a part of PhD thesis of the first author. The authors thank to The Scientific and Technological Research Council of Turkey (TUBITAK – the grant number is 111M065), Yildiz Technical University Scientific Research Projects Coordination Department (the grant number is 2011-10-01-KAP03) and Turkish Academy of Sciences (TUBA) for their financial supporting.

References

[1] Wang Y, Zeng S, Huang J. Experimental investigation of applying Miller cycle to reduce NOx emission from diesel engine. Proc. IMechE, Part A J. Power Energy 2005;219:631–8.
[2] Wang Y, Lin L, Zeng S. Application of the Miller cycle to reduce NOx emissions from petrol engines. Appl Energy 2008;85:463–74.

[3] Wang Y, Lin L, Roskilly AP. An analytic study of applying Miller cycle to reduce NOx emission from petrol engine. Appl Therm Eng 2007;27:1779–89.
[4] Mikalsen R, Wang YD, Roskilly AP. A comparison of Miller and Otto cycle natural gas engines for small scale CHP applications. Appl Energy 2009;86:922–7.
[5] Gonca G. Investigation of the effect of steam injection on performance and emissions in a turbocharged diesel engine running with the Miller cycle. 2013. PhD Thesis.
[6] Gonca G, Sahin B, Ust Y, Parlak A, Safa A. Comparison of steam injected diesel engine and Miller Cycled diesel engine by using two zone combustion model. J Energy Inst; 2014, 1–10, doi:10.1016/j.joei.2014.04.007 [in press].
[7] Gonca G, Sahin B, Ust Y, Parlak A. A study on late intake valve closing Miller Cycled diesel engine. Arab J Sci Eng 2013;38:383–93.
[8] Gonca G, Sahin B, Ust Y. Performance maps for an air-standard irreversible Dual-Miller cycle (DMC) with late inlet valve closing (LIVC) version. Energy 2013;5:285–90.
[9] Al-Sarkhi A, Jaber JO, Probert SD. Efficiency of a Miller engine. Appl Energy 2006;83:343–51.
[10] Al-Sarkhi A, Al-Hinti I, Abu-Nada E, Akash B. Performance evaluation of irreversible Miller engine under various specific heat models. Int Commun Heat Mass 2007;34:897–906.
[11] Al-Sarkhi A, Akash BA, Jaber JO. Efficiency of Miller engine at maximum power density. Int Commun Heat Mass 2002;29:1159–67.
[12] Zhao Y, Chen J. Performance analysis of an irreversible Miller heat engine and its optimum criteria. Appl Therm Eng 2007;27:2051–8.
[13] Ebrahimi. Thermodynamic modeling of performance of a Miller cycle with engine speed and variable specific heat ratio of working fluid. Comput Math Appl 2011;62:2169–76.
[14] Ebrahimi. Performance analysis of an irreversible Miller cycle with considerations of relative air–fuel ratio and stroke length. Appl Math Model 2012;36:4073–9.
[15] Rinaldini CA, Mattarelli E, Golovitchev VI. Potential of the Miller cycle on a HSDI diesel automotive engine. Appl Energy 2013;112:102–19.
[16] Li T, Gao Y, Wang J, Chen Z. The Miller cycle effects on improvement of fuel economy in a highly boosted, high compression ratio, direct-injection gasoline engine: EIVC vs LIVC. Energy Convers Manage 2014;79:59–65.
[17] Wu C, Puzinauskas PV, Tsai JS. Performance analysis and optimization of a supercharged Miller cycle Otto engine. Appl Therm Eng 2003;23:511–21.
[18] Ge Y, Chen L, Sun F, Wu C. Reciprocating heat-engine cycles. Appl Energy 2005;81:397–408.
[19] Parlak A, Ayhan V, Üst Y, Sahin B, Cesur Y, Boru B, Kökkülünk G. New method to reduce NOx emissions of diesel engines: electronically controlled steam injection system. J Energy Inst 2012;85:135–9.
[20] Kokkulunk G, Gonca G, Parlak A. The effects of design parameters on performance and no emissions of steam-injected diesel engine with exhaust gas recirculation. Arab J Sci Eng 2014;39(5):4119–29.
[21] Cesur I, Parlak A, Ayhan A, Gonca G, Boru B. The effects of electronic controlled steam injection on spark ignition engine. Appl Therm Eng 2013;55:61–8.
[22] Kokkulunk G, Gonca G, Ayhan V, Cesur I, Parlak A. Theoretical and experimental investigation of diesel engine with steam injection system on performance and emission parameters. Appl Therm Eng 2013;54:161–70.
[23] Gonca G, Sahin B, Ust Y, Parlak A. Determination of the optimum temperatures and mass ratios of steam injected into turbocharged internal combustion engines. J Renew Sustain Energy 2013;023119(5):1–13. http://dx.doi.org/10.1063/1.4798313.
[24] Gonca G. Investigation of the effects of steam injection on performance and NO emissions of a diesel engine running with ethanol–diesel blend. Energy Convers Manage 2014;77:450–7.
[25] Parlak A, Ayhan V, Cesur I, Kokkulunk G. Investigation of the effects of steam injection on performance and emissions of a diesel engine fuelled with tobacco seed oil methyl ester. Fuel Process Technol 2013;116:101–9.
[26] Ayhan V. Investigation of the effects of steam injection into the diesel engine on NOx and PM emissions. Sakarya University; 2009. PhD thesis.
[27] Ferguson R. Internal combustion engines applied thermosciences. New York: John Wiley & Sons Inc.; 1986.
[28] Hohenberg G. Advanced approaches for heat transfer calculations. SAE J Automot Eng 1979:790825.
[29] Sitkei G. Kraftstoffaufbereitung und Verbrennung bei Dieselmotoren. Berlin: Springer Verlag; 1964.
[30] Miyamoto N, Chikahisa T, Murayama T, Sawyer R. Description and analysis of diesel engine rate of combustion and performance using Wiebe's functions. SAE 1985:850107.
[31] Heywood JB. Internal combustion engine fundamentals. New York: McGraw-Hill Inc.; 1998.
[32] Olikara C, Borman G. A computer program for calculating properties of equilibrium combustion products with some applications to the engines. SAE J Automot Eng 1975:750468.
[33] Kokkulunk G, Parlak A, Ayhan V, Cesur I, Gonca G, Boru B. Theoretical and experimental investigation of steam injected diesel engine with EGR. Energy 2014;74:331–9.
[34] Gonca G, Sahin B, Parlak A, Ust Y, Ayhan V, Cesur I, et al. Theoretical and experimental investigation of the Miller cycle diesel engine in terms of performance and emission parameters. Appl Energy 2015;138:11–20.